Analysis of the View Factors in Rooftop PV Solar

Yasser F. Nassar
Dept. of Mechanical and Industrial Engineering
Sebha University
Brack, Libya
yas.nassar1@sebhau.edu.ly

Said Belhaj
Center for Solar Energy Research and Studies
Tripoli, Libya
sbelhaj@csers.ly

Samer Y. Alsadi
Dept. of Electrical Engineering
Palestine Technical Univ.-Kadoorie
Tulkarm-Palestine
s.alsadi@ptuk.edu.ps

hkhozondar@iugaza.edu.ps

Hala J. El-Khozondar
Dept. of Electrical Engineering and smart systems
Islamic University of Gaza
Gaza, Palestine

2022 3rd International Conference on Smart Grid and Renewable Energy (SGRE) | 978-1-6654-7908-0/22/$31.00 ©2022 IEEE | DOI: 10.1109/SGRE53517.2022.9774104

***Abstract* - In solar PV fields, solar photovoltaic panels are typically arranged in parallel rows one after the other. This arrangement introduces variations in the distribution of solar irradiance over the entire field, compared to measurements made at meteorological weather stations and data obtained from solar radiation databases. This is due to the difference in the view factors between the rows of the solar PV field and a single reference surface, as well as the presence of shade on rear rows and in the space separating the rows. These phenomena combined will reduce the energy yield of a solar PV field. Accurate estimation of solar radiation on solar fields requires knowledge of the sky, ground, and rear surface of the preceding row view factors, and an estimation of the time and space occupied by the row's shadow. Prior literature has addressed this issue using two-dimensional (2D) techniques such as Crossed-Strings Method, which this study proved to be inaccurate particularly in the case of Rooftop solar PV fields. This study uses a novel three-dimensional (3D) analytical and numerical analysis to determine the view factors associated with solar fields using hourly solar irradiance data acquired from Solar-GIS for the period 2007-2020, including global, beam, and sky diffuse irradiance components on horizontal plane. The study uses both isotropic and anisotropic transposition analyses to determine solar irradiance incident on the solar field with varying tilt angles of solar panels and distance separating the rows.**

Index Terms* - *PV Solar field, view factor, sky view factor, ground view factor, rooftop solar PV

I. Introduction

With the exception of the first row in a solar field, it is not well known that the total solar radiation incident on the rest of the solar field consists of four components; beam, sky diffuse, ground reflected, and radiation reflected from the back of the front rows [1,2]. Arranging solar fields in rows one after the other inevitably results in uneven intensity of solar radiation over the entire field, which is not reflected in meteorological databanks and is not accounted for in traditional transposition models in the calculation of irradiance on an inclined plane [3]. The inherent differences in the sky and ground view factors amongst the solar field rows and the presence of shadows in the space separating the rows make the handling of ground-albedo for the entire solar field more complex than it would for a single row array or the first row of a solar field, as was discussed in several experimental [4] and theoretical research studies [5].

View factors are widely used in radiative heat transfer analysis of many energy engineering applications. An on-line compilation of view factors for over 300 common geometries is provided by Howell [6], and the list is regularly updated with new geometries. Nassar recently developed a numerical model that facilitates the simulation of all types of solar fields [7]. Most studies relating to view factors were reviewed in [8]. View factors of photovoltaic collectors on roof tops of buildings were reported in [9], and view factors of solar collectors deployed on horizontal, inclined and step-like planes were discussed in [5]. All previously maintained studies addressed the solar PV field as a two-dimensional problem. In general, two-dimensional analysis is based on the hypothesis that the length of a row is infinitely longer than its height [9]. Although this assumption might be considered reasonable for large solar PV fields, the same cannot be said for rooftop solar PV installations. The installation of solar PV on roof-tops of buildings is becoming more widespread and can be a solution to the energy problem in many countries [10,11].

The view factors of the sky and the ground as seen by the rows of solar PV field has typically been calculated by means of Crossed-String Method (CSM) [4,5,8]. What distinguishes this study from its predecessors is the use of three-dimensional analysis to address the problem comprehensively, making it applicable to any type of solar field. A key finding of this work is the outline of two approaches to estimate solar irradiance incident on solar field rows for isotropic and anisotropic skies, something that has not thus far been studied, to the best of our knowledge. This represents the significance of the present research.

II. Mathematical Modelling of View Facors

A. Definition and Algebra of View Factors

The view factor $F_{A_i-A_j}$ is defined as the fraction of radiation leaving surface A_i that is directly striking surface A_j. Knowledge of basic view factor algebra is necessary for analysing and solving view factor problems, some of which are [12]:

The reciprocity rule: $$A_i F_{A_i-A_j} = A_j F_{A_j-A_i} \quad (1)$$

The summation rule: $$\sum_{j=1}^{N} F_{A_i-A_j} = 1 \quad (2)$$

The superposition rule: $$F_{A_i-(A_{j1}+A_{j2})} = F_{A_i-A_{j1}} + F_{A_i-A_{j2}} \quad (3)$$

B. Two-Dimensional approach for calculation of view factors

One of the most widely used methods for two-dimensional analysis of view factors is Crossed Strings Method (CSM). CSM is applicable to geometries that are very long in one direction relative to the other directions. By attaching strings

between corners, as illustrated in Fig. 1, CSM can be expressed as [5]:

$$F_{i\to j} = \frac{\sum crossed\ strings - \sum uncrossed\ strings}{2 \times string\ on\ surface\ i} \quad (4)$$

According to this definition, the view factors may be written as:

$$F_{A_1\to s} = \frac{1+cos\beta}{2} \quad (5)$$

$$F_{A_2\to s} = \frac{1}{2}\left[1+\frac{d}{W}-\sqrt{\left(\frac{d}{w}-cos\beta\right)^2+(sin\beta)^2}\right] \quad (6)$$

Where: $F_{A_1\to s}$ is 1st row to sky view factor, $F_{A_1\to s}$ is 1st row to ground view factor, $F_{A_2\to s}$ is 2nd row to sky view factor, $F_{A_2\to g}$ is 2nd row to ground view factor, and $F_{A_1\to A_{1r}}$ is 2nd row to rear-surface of the 1st row view factor, β is the surface tilt angle and d presents the distance separating the rows, W is row's hight and the fraction $\frac{d}{W}$ presents the aspect ratio.

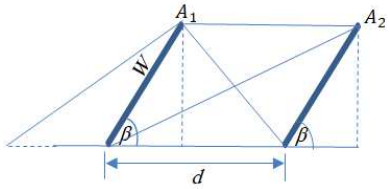

Fig. 1 Definition of crossed-strings method for two surfaces of infinite length

Fig.2 illustrates a comparison between the 2nd row surface view factors for different design parameters, for CSM and 3D analysis

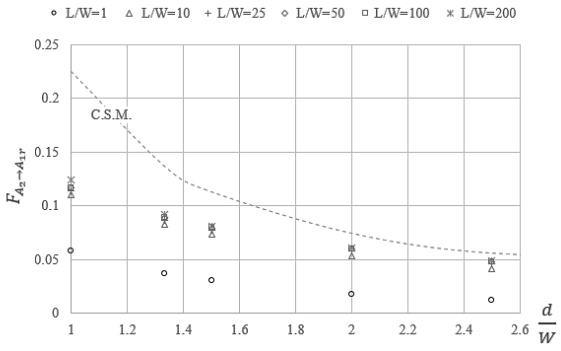

Fig.2. Comparison of view factors of surface F_{A_2} obtained by CSM and 3D analysis as a function of aspect ratio d/W for various aspect ratios L/W and β=30°

Error in the estimation of view factors is calculated using the formula:

$$Error\% = \frac{F_{A_2}\ (CSM) - F_{A_2}\ (3D)}{F_{A_2}\ (CSM)} \times 100 \quad (7)$$

For solar field with aspect ratios $\frac{d}{W} \approx 1.5$ and $\frac{L}{W} \approx 25$, the view factors estimates showed errors of 3%, -1% and 44% for $F_{A_1\to s}$, $F_{A_2\to g}$ and $F_{A_2\to A_{1r}}$, respectively. In the case of rooftop solar PV installations with aspect ratios $\frac{d}{W} \approx 1.5$ and $\frac{L}{W} \approx 5$, the errors were found to be 30%, -6% and 38% for $F_{A_1\to s}$, $F_{A_2\to g}$ and $F_{A_2\to A_{1r}}$, respectively. It should be noted that CSM produced a large $F_{A_2\to A_{1r}}$ error even for vertical planes compared with 3-D analysis. Applying eq (10) for the same solar field ($\frac{d}{W} \approx 1.5$ and $\frac{L}{W} \approx 25$), the errors produced were 0.4% for 3D method [8] and -11% for CSM.

The inherent restriction of CSM where the length of a solar field is assumed to be much longer than its width (i.e. $\frac{L}{W} \cong \infty$) is applicable only in large solar PV fields >100 MW. In comparison, smaller solar PV fields such as rooftop installation where the aspect ratio $\frac{L}{W}$ is relatively small (<5), the view factors estimates exhibit significantly larger errors.

C. Three-Dimensional approach for calculation of view factors

In order to achieve improved predictions of energy yield, costs, and ensure optimum design, it is necessary to adopt a 3-D analysis approach to accurately calculate view factors of solar PV fields. Fig.3, shows two solar collectors placed one behind the other to represent a solar PV field, indicating all the view factors associated with it, serving as a reference for the remaining discussion in this paper. It also presents the nomenclature of view factors that take place in a horizontal-plan fixed-mode solar PV field at any moment of time.

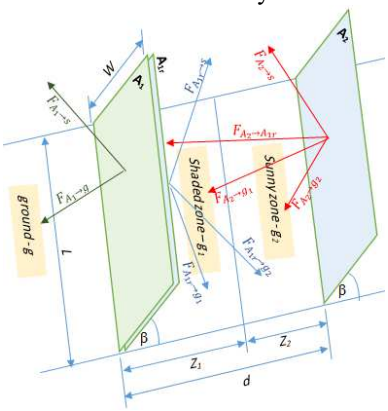

Fig.3 View factors of a horizontal plane solar PV field at an instant of time

The view factors expressions presented in references [6,7] can be rewritten to match the geometry of the solar PV field depicted in Fig.3. It should be noted that these multi-integration expressions have no mathematical solution and will require the use of numerical techniques to evaluate them. The 4th order integral has been solved numerically by Nassar by means of Simpson's 1/3 rule [7]. While other integrats are partially solved with one term remaining unsolved. The unsolved term is solved in this work numerically by means of Gaussian Quadrature 5 points rule.

D. Calculation of shadow in space separating rows

Shadow plays an important role in determining the ground view factor for the 2nd and subsequent rows. The space that separates the rows can be divided into two parts, shaded and unshaded zones. Estimation of shadow in solar fields has been studied extensively [13, 14]. Alsadi and Nassar developed a general expression for shadow geometry in all types of solar fields [15].

Since the length of the shadow in the space separating the rows is much longer than its width, it can be assumed that the shadow is of rectangle shape, which will have the effect of simplifying the problem without significant effect on the results. Fig.4 depicts the graphical representation of the derivation of expressions for shaded and unshaded zones. The

expressions that represent the length of shaded g_1 and unshaded g_2 zones shown in Fig. 4 can be written in the form of dimensionless ratio of lengths Z_1 and Z_2 of shaded and unshaded zones, respectively, to the distance separating the rows (d), to give the following equations:

$$\frac{Z_1}{d} = \frac{W}{d}cos\beta + \frac{W}{d}\frac{sin\beta}{tan\alpha}cos(\emptyset - \psi) \qquad if \begin{cases} \frac{Z_1}{d} < 0; & \frac{Z_1}{d} = 0 \\ \frac{Z_1}{d} > 1; & \frac{Z_1}{d} = 1 \end{cases} \quad (8)$$

$$\frac{Z_2}{d} = 1 - \frac{Z_1}{d} \qquad if \begin{cases} \frac{Z_2}{d} < 0; & \frac{Z_2}{d} = 0 \\ \frac{Z_2}{d} > 1; & \frac{Z_2}{d} = 1 \end{cases} \quad (9)$$

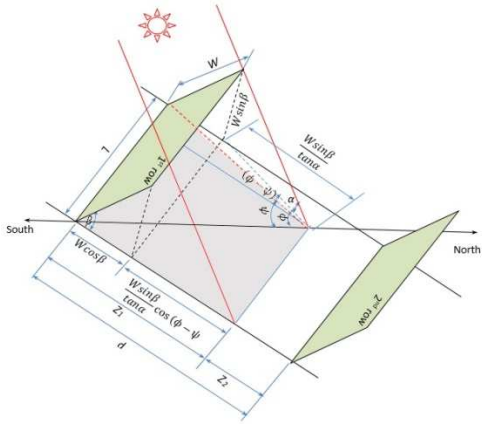

Fig.4. Graphical representation of shaded and unshaded zones in a solar field

III. METHODOLOGY

The methodology begins with calculating all view factors of first and second rows, in additional to calculating the shadding occurring between the spaces separat the rows. The followed approach can be outlined in the following steps:

A. First row view factors

The first row of a solar field can be thought of as a single tilted surface for the purpose of determining the view factors associated with it and solar radiation incident upon it. The first row view factors include two factors, those are:

1. First row-Ground view factor; $F_{A_1 \to g}$

The subscript g refers to ground surface seen by the first row surface A_1, assuming the ground surface in front and on either side of the first row is unshaded. Accordingly, the value of $F_{A_1 \to g}$ is constant and it is effected only by the tilt angle β. And it is directly proportional to the tilt angle β.

2. First row-Sky view factor; $F_{A_1 \to s}$

The value of $F_{A_1 \to s}$ is constant, and it effected only by the row tilt angle β. And it is $F_{A_1 \to s}$ is inversely proportional to the tilt angle β.

B. Second row view factors

In general, the second row view factors include four factors, those are:

1. Second row- reae surface of first row view factor*;* $F_{A_2 \to A_{1r}}$

The view factor $F_{A_2 \to A_{1r}}$ represents the 2nd row to rear surface of the 1st row view factor.

2. Second row-ground view factor; $F_{A_2 \to (g_1 + g_2)}$

The subscripts g_1 and g_2 refer to the shaded and unshaded zones, respectively. The value of $F_{A_2 \to (g_1 + g_2)}$ is constant, and depending on solar field design parameters β and d.

3. Second row-sky view factor; $F_{A_2 \to sky}$

The sky view factor is considered one of the most important factors due to its relatively large effect on the contribution of sky-diffuse irradiance to the total global solar radiation. The value of $F_{A_2 \to sky}$ can be obtained by applying the superposition rule. The second row sees the sky as the first row sees it ($F_{A_1 \to sky}$) less the blocking that takes place due to the presence of the first row in front of it ($F_{A_2 \to A_{1r}}$).

4. Second row-ground view factor; $F_{A_2 \to g}$

The subscript g refers to ground seen by row, in front and on either side of it. Its value is obtained using the summation rule, by subtracting the total second row view factors from that of the first. We assume that the total ground area in this case is unshaded.

C. Dynamic view factors

Four view factors are classified as dynamic view factors; this is because they are dependent on the shadow that occurs in the space separating the rows. Shadow, in turn, depends on time and location hence the name "dynamic". These view factors are: $F_{A_2 \to g_1}$, $F_{A_2 \to g_2}$, $F_{A_{1r} \to g_1}$ and $F_{A_{1r} \to g_2}$. They are respectively: view factor between the 2nd row and the shaded zone g_1, view factor between the 2nd row and the unshaded zone g_2, view factor between rear surface of the 1st row and shaded zone g_1, and view factor between rear surface of the 1st row and unshaded zone g_2, as illustrated in Fig. 3.

D. Calculation of Shadow

Shadow is strongly dependent on the design parameters, location (∅) and time represented by solar altitude and azimuth angles α and γ respectively. It is a well known fact that shadow is longer at high latitudes, early in the morning and late in the evening, reaching its longest in winter solstice. Conversely, it is shorter at solar noon, reaching its shortest at summer solstice, according to the approach that prescribed by Alsadi and Nassar in [15].

IV. RESULTS AND DISCUSSIONS

Fig.5 illustrates the relationship between the view factor $F_{A_2 \to A_{1r}}$ and design parameters of a solar PV field in contour forms.

Fig.5 shows that increasing the tilt angle β leads to a significant increase in the view factor $F_{A_2 \to A_{1r}}$ by a cubic order polynomial. Similarly, an increase in the value of $F_{A_2 \to A_{1r}}$ is almost proportional to that of the aspect ratio $\frac{W}{d}$. On the other hand, the influence of aspect ratio $\frac{L}{W}$ is limited to values <10 as in the case of rooftop solar installation.

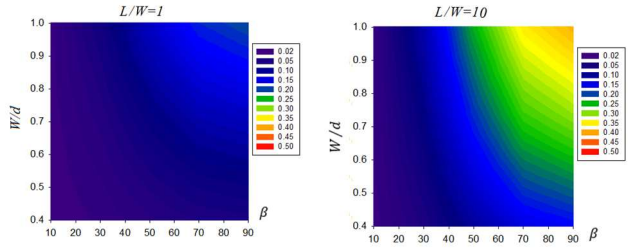

Fig. 5. Contour representation of $F_{A_2 \to A_{1r}}$ as a function of aspect ratio $\frac{W}{d}$ and row tilt angle β, for various values of aspect ratio $\frac{L}{W}$.

The effect of solar field design parameters on the value of $\boldsymbol{F_{A_2 \to (g_1+g_2)}}$ is depicted as contour plot in Fig. 6.

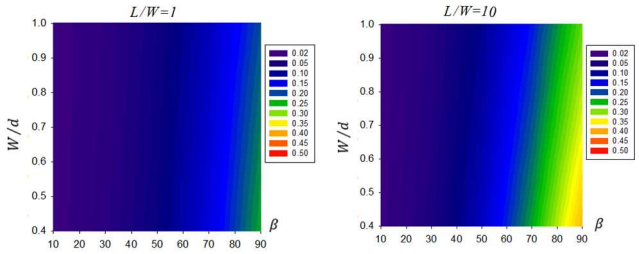

Fig. 6. Contour representation of $\boldsymbol{F_{A_2 \to (g_1+g_2)}}$ as a function of aspect ratio $\frac{W}{d}$ and row tilt angle β, for various values of aspect ratio $\frac{L}{W}$.

Fig. 6 shows that increasing row tilt angle β leads to an increase in view factor $F_{A_2 \to (g_1+g_2)}$ with a quadratic power polynomial scale. It also shows that increasing the value of aspect ratio $\frac{W}{d}$ leads to a linear decrease in the value of $F_{A_2 \to (g_1+g_2)}$. On the other hand, increasing the length of the row for aspect ratio $\frac{L}{W} < 10$ leads to a large logarithmical scale increase in the value $F_{A_2 \to (g_1+g_2)}$, flattening beyond $\frac{L}{W} > 10$ into a straight line having zero slope.

Fig. 7 is a contour plot showing the behaviour of $F_{A_2 \to sky}$ when changing the design parameters of the solar PV field β, $\frac{W}{d}$ and $\frac{L}{W}$.

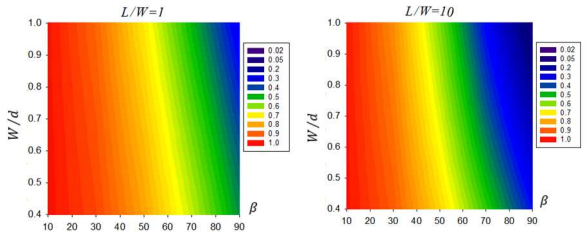

Fig.7: Contour representation of $F_{A_2 \to sky}$ as a function of $\frac{W}{d}$, β and $\frac{L}{W}$.

The row tilt angle is a critical parameter in the sky view factor such that increasing the row tilt angle leads to a reduction of the value of sky view factor by a cubic order polynomial. Conversely, the value of sky view factor is inversely proportional to the aspect ratio $\frac{W}{d}$. The length of row, on the other hand, has an inverse power effect for low aspect ratio $\frac{L}{W} < 10$, diminishing to have no effect for larger aspect ratios.

Fig. 8 is a contour plot representing the relationship between the $F_{A_2 \to g}$ and the solar PV field's design parameters β, $\frac{W}{d}$ and $\frac{L}{W}$.

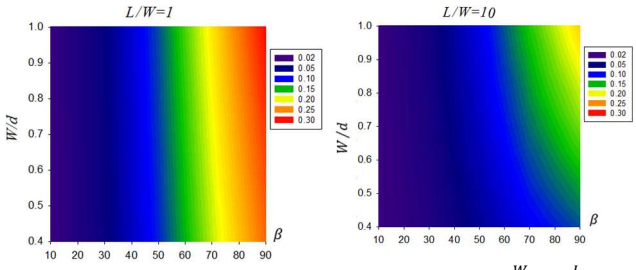

Fig.8: Contour presentation of $F_{A_2 \to g}$ as a function of β, $\frac{W}{d}$ and $\frac{L}{W}$.

$F_{A_2 \to g}$ is significantly affected by tilt angle β, having almost direct linear relationship. With respect to the aspect ratio $\frac{L}{W}$, the view factor $F_{A_2 \to g}$ has a power function relationship where increasing $\frac{L}{W}$ for ratios <10 leads to a sharp decrease in $F_{A_2 \to g}$, diminishing to no effect for larger ratios. On the other hand, the aspect ratio W/d has a lesser effect being almost direct proportion to $F_{A_2 \to g}$.

Defining shadow as it relates to solar PV fields depends on field dimensions and row tilt angle as well location and time. Of these parameters, however, row tilt angle β is considered the most weighted and flexible parameter to control in order to influence the effect of shadow. Vokony and et. al. recommended tilt angles for European installations not to exceed 30° [16], while a tilt angle of about 20° was recommended for North Africa [17,18]. Fig. 9 is a radar plot representing a comparison between two categories of locations: MENA with $\emptyset = 30°, \beta = 20°$ and Europe with $\emptyset = 40°, \beta = 30°$ for both longest and shortest shadows occurring on June 21st and December 21st respectively, for several aspect ratios $\frac{W}{d} = 0.5, 0.67$ and 1.0.

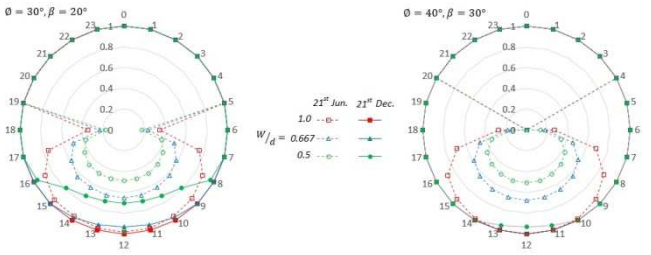

Fig. 9: Comparison of shadow zone length ratio $\frac{Z_1}{d}$ between two locations with different tilt angles on the 21st of Summer and Winter Solstices. The aspect ratio $\frac{W}{d}$ is a parameter

V. A CASE STUDY

The results presented here are for a horizontal-plane fixed-mode solar PV field project planned by the Libyan government in an effort to transition to electricity generation using abundant renewable energy resources available in the country. The project is located on the outskirts of the capital city Tripoli $(32.815°N, 13.439°E)$. The solar PV field is orientated due south $(\psi = 0)$, having a tilt angle $\beta = 20°$ from the horizontal , the rows dimensions $L \times W$ are 200×6 m, with the rows placed 9 m apart.

Applying the above maintioned approach for the above solar field yielded the results depicted in Fig. 10 represented

as radar chart for the 21st of every month for both shaded and unshaded zones.

View factor of second row; F_{A_2}

second row- rear surface of first row view factor; $F_{A_2 \to A_{1r}}$

The view factor $F_{A_2 \to A_{1r}}$ was determined by solving the multi-integral equation. A modified version of FORTRAN code developed by Nassar [7] was used to numerically evaluate the view factor $F_{A_2 \to A_{1r}}$.

$$F_{A_2 \to A_{1r}} = 0.02444224 \tag{10}$$

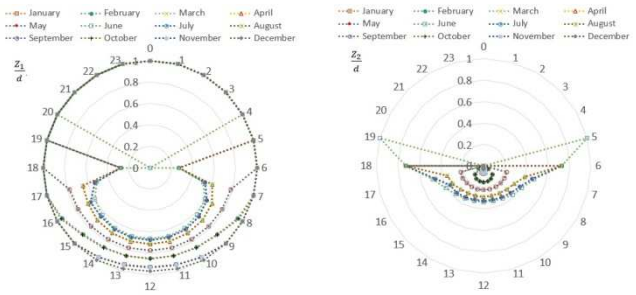

Fig.10. Aspect ratio of shaded and unshaded zones $\frac{Z_1}{d}$ and $\frac{Z_2}{d}$ for the 21st of every month for given design parameters
$\emptyset = 32.815°N, \psi = 0, \beta = 20°,\ L \times W = 200 \times 6\ m$ and $d = 9.0\ m$

Second row- sky view factor; $F_{A_2 \to s}$

The view factor $F_{A_2 \to s}$ is a constant value and it dependents only on design parameters. $F_{A_2 \to s}$ has been obtained by applying the superposition rule. The second and subsequent rows see the sky in the same manner as the first row ($F_{A_1 \to s}$) less the blocking that takes place due to the presence of the first row ($F_{A_2 \to A_{1r}}$), given by:

$$F_{A_2 \to s} = F_{A_1 \to s} - F_{A_2 \to A_{1r}} = \frac{1 + cos\beta}{2} - F_{A_2 \to A_{1r}} \tag{11}$$
$$F_{A_2 \to s} = 0.969846 - 0.02444224 = 0.9454041$$

Second row- space separating rows view factor; $F_{A_2 \to (g_1 + g_2)}$

The view factor $\boldsymbol{F_{A_2 \to (g_1 + g_2)}}$ is a constant value dependent only on design parameters. This view factor represents the view factor between surface of second row and space separating rows ($Z_1 + Z_2$). The value of $F_{A_2 \to (g_1 + g_2)}$ for given solar PV field characteristics was found to be:

$$F_{A_2 \to (g_1 + g_2)} = 0.0178627 \tag{12}$$

Second row- sunny zone view factor; $F_{A_2 \to g_2}$

The value of view factor $F_{A_2 \to g_2}$ is obtained either by applying eq. (9) or in the same manner as calculating $F_{A_2 \to (g1+g2)}$ substituting the length of unshaded zone Z_2 for d such that the aspect ratio become $\frac{W}{Z_2}$ and $\frac{L}{Z_2}$.

Second row- shaded zone view factor; $F_{A_2 \to g_1}$

The view factor $F_{A_2 \to g_1}$ is calculated directly from the superposition rule by subtracting $F_{A_2 \to g_2}$ from $F_{A_2 \to (g_1 + g_2)}$, giving:

$$F_{A_2 \to g_1} = F_{A_2 \to (g_1 + g_2)} - F_{A_2 \to g_2} \tag{13}$$

The dynamic values of $F_{A_2 \to g_1}$ and $F_{A_2 \to g_2}$ are depicted in the form of radar chart in Fig. 11 for the 21st of every month. Since the values of $F_{A_2 \to g_1}$ and $F_{A_2 \to g_2}$ are complementary and dependent on shaded and unshaded profiles, increasing the shadow length leads to an increase in $F_{A_2 \to g_1}$ and a decrease in $F_{A_2 \to g_2}$, and vice versa. The symmetry of the two profiles can be observed in Fig. 11.

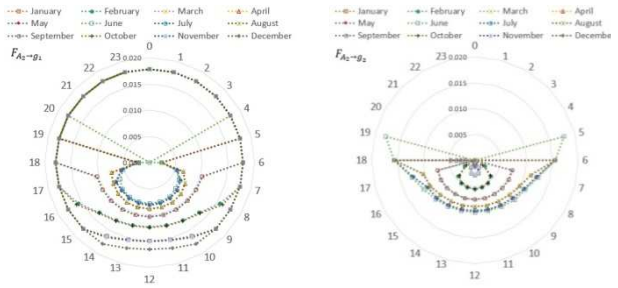

Fig. 11 Hourly values of $F_{A_2 \to g_1}$ and $F_{A_2 \to g_2}$ for the 21st of every month

Second row- surrounding ground view factor; $F_{A_2 \to g}$

The subscription $\boldsymbol{g}$ refers to the ground surrounding the second, not including the space separating the rows ($g_1 + g_2$) and assumed to be unshaded. The value of $F_{A_2 \to g}$ is obtained by applying the summation rule:

$$F_{A_2 \to g} = 1 - \left(F_{A_2 \to (g_1 + g_2)} + F_{A_2 \to sky} + F_{A_2 \to A_{1r}}\right)$$
$$F_{A_2 \to g} = 1 - (0.0178627 + 0.9454041 + 0.02444224) = 0.0122939 \tag{14}$$

Rear surface of first row- space separating rows view factor; $F_{A_{1r} \to (g1+g_2)}$

The view factor $F_{A_{1r} \to (g1+g_2)}$ is a constant value dependent only on design parameters. It is determined and found as:

$$F_{A_{1r} \to (g1+g_2)} = 0.9175759 \tag{15}$$

Second row- sunny zone view factor; $F_{A_{1r} \to g_2}$

The view factor between rear surface of first row and unshaded zone g_2 is obtained by using view factor algebra summation rule eq. (2) by subtracting the value of $F_{A_{1r} \to g_1}$ from the view factor of the total space separating the rows $F_{A_{1r} \to (g1+g_2)}$.

$$F_{A_{1r} \to g_2} = F_{A_{1r} \to (g_1 + g_2)} - F_{A_{1r} \to g_1} \tag{16}$$

The dynamic values of $F_{A_{1r} \to g_1}$ and $F_{A_{1r} \to g_2}$ are depicted in the form of radar charts in Fig. 12 for the 21st of every month. The value of $F_{A_{1r} \to g_1}$ is high at low tilt angles, influenced largely by the width of shaded zone Z_l. The relationship is clearly demonstrated by the similarities between Fig. 12 in that the value of $F_{A_{1r} \to g_1}$ goes up with an increase in width of shaded zone Z_l and vice versa.

Rear surface of first row-surrounding ground view factor; $F_{A_{1r} \to g}$

The view factor $F_{A_{1r} \to g}$ is treated in the same way as with sky view factor of second row $F_{A_2 \to sky}$ using the superposition rule. The rear surface of first row sees the

surrounding ground in the same manner as the first row sees the sky ($F_{A_1 \to s}$) less the blocking that takes place due to the presence of the second row ($F_{A_2 \to A_{1r}}$) and the space separating the rows, giving:

$$F_{A_{1r} \to g} = \frac{1 + cos\beta}{2} - \left(F_{A_{1r} \to (g_1 + g_2)} + F_{A_2 \to A_{1r}}\right)$$
$$F_{A_{1r} \to g} = 0.96984631 - (0.9175759 + 0.02444224) = 0.02782817 \quad (17)$$

This value represents what the row sees from the ground surrounding the row, assumed to be unshaded.

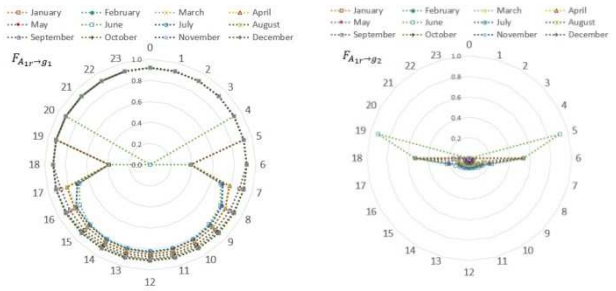

Fig. 12: Hourly values of $F_{A_{1r} \to g_1}$ and $F_{A_{1r} \to g_2}$ for the 21st of every month.

Rear surface of first row- sky view factor; $F_{A_{1r} \to s}$

The view factor $F_{A_{1r} \to s}$ is a constant value dependent only on design parameters and treated in the same manner as $F_{A_2 \to g}$ using the summation rule, giving:

$$F_{A_{1r} \to s} = 1 - (F_{A_1 \to g} + F_{A_1 \to (g_1 + g_2)} + F_{A_2 \to A_{1r}})$$
$$F_{A_{1r} \to s} = 1 - (0.02782817 + 0.9175759 + 0.024442243 = 0.0301537 \quad (18)$$

VI. CONCLUSIONS

This research used 3D numerical analysis to calculate the view factors of a horizontal plane fixed mode solar PV field. However, it can equally be applied to all types of solar fields, including rooftops and building façades. It only requires defining the view factors between the PV panels and the environment. The influence of the design parameters, location and time are analysed. The present study shows that the tilt angle has a higher weighting compared to other design parameters. The key finding of this research is improved accuracy of estimation of solar PV field potential by introducing a model for estimating reduction in solar irradiance incident on the 2nd and subsequent rows relative to the first row of a solar field. The obtained results showed that reduction in solar irradiance is higher at high latitudes, reaching 2.3%. In addition, the reduction in solar irradiance is high under overcast sky conditions, reaching 17% at high latitudes and up to 5% in North Africa region, and 30% reduction in solar radiation for shaded zones. It is highly advisable that shading in solar fields be avoided where possible with measures such as reducing the tilt angle and/or increasing the distance separating the rows. Although, the later measure has some economic implications which need to be considered.

Aknowlegement: Authors would like to thank Palestine Technical University – Kadoorie for their cooperation and support this research.

REFERENCES

[1] Nassar Y., Solar Energy Engineering-Active Applications, Sebha University, Libya, 2006

[2] Alsadi S., Nassar Y., (2017) A Numerical Simulation of a Stationary Solar Field Augmented by Plane Reflectors: Optimum Design Parameters. Smart Grid and Renewable Energy, 8, pp. 221-239. https://doi.org/10.4236/sgre.2017.87015

[3] Nassar Y., Hafez A., Alsadi S., (2020) Multi-Factorial Comparison for 24 Distinct Transposition Models for Inclined Surface Solar Irradiance Computation in the State of Palestine: A Case Study. Front. Energy Res. 7: 163. https://doi.org/10.3389/fenrg.2019.00163

[4] Alsadi S., Nassar Y., (2017) Estimation of Solar Irradiance on Solar Fields: An Analytical Approach and Experimental Results," in *IEEE Transactions on Sustainable Energy*, vol. 8, no. 4, pp. 1601-1608, Oct. 2017, https://doi.org/10.1109/TSTE.2017.2697913.

[5] Nassar Y., Alsadi S., (2016) View Factors of Flat Solar Collectors Array in Flat, Inclined, and Step-Like Solar Fields. ASME. *J. Sol. Energy Eng.*; 138(6): 061005. https://doi.org/10.1115/1.4034549 .

[6] Howell J., (2016) A catalog of radiation heat transfer configuration factors, http://www.thermalradiation.net/indexCat.html

[7] Nassar Y., (2020) Analytical-Numerical Computation of View Factor for several arrangements of two rectangular surfaces with non-common edge, International journal of heat and mass transfer, 159,120130, https://doi.org/10.1016/j.ijheatmasstransfer.2020.120130

[8] Appelbaum J., (2018) The role of view factors in solar photovoltaic fields, Renewable and Sustainable Energy Reviews, vol.81, pp. 161-171. https://doi.org/10.1016/j.rser.2017.07.026

[9] Appelbaum J, Aronescu A. (2016) View factors of photovoltaic collectors on roof tops. J Renew Sustain Energy, 8:025302

[10] Nassar Y., Alsadi S., (2019). Assessment of solar energy potential in Gaza Strip-Palestine, Sustainable Energy Technologies and Assessments 31, 318–328. https://doi.org/10.1016/j.seta.2018.12.010

[11] Awad H., Nassar Y., Hafez A., Sherbiny M., Ali A., (2021). Optimal design and economic feasibility of rooftop photovoltaic energy system for Assuit University, Egypt, Ain Shams Engineering Journal. https://doi.org/10.1016/j.asej.2021.09.026

[12] Baehr, H., Karl S., Heat and Mass Transfer, 3rd ed., Springer, Berlin, Heidelberg, p. 588. 2011

[13] Groumpos P., Khouzam K., (1987) A generic approach to the shadow effect of large solar power systems, Solar Cells, 22:1, 29-46. https://doi.org/10.1016/0379-6787(87)90068-8

[14] Nassar Y., Hadi H., , Salem A., (2008) Time Tracking of the Shadow in the Solar Fields, Journal of Sebha University, (7) 2, pp. 59-73.

[15] Alsadi S., Nassar Y., (2019) A general expression for the shadow geometry for fixed mode horizontal, step-like structure and inclined solar fields, Solar Energy, 181, 53–69, https://doi.org/10.1016/j.solener.2019.01.090

[16] Vokony I., Hartmann B., Talamon A., Viktor R., (2018) On Selecting Optimum Tilt Angle for Solar Photovoltaic Farms, International journal of renewable energy research, Vol.8, No.4,1926-1935. https://pdfs.semanticscholar.org/6a8f/239e33d25a741bfd1e05af339a7a3fc85f6e.pdf

[17] Nassar Y., Abdunnab M., Sbea M., Hafez M., Amer K., Ahmed A.. Belgasim B., (2021). Dynamic analysis and sizing optimization of a pumped hydroelectric storage-integrated hybrid PV/Wind system: A case study," *Energy Conversion and Management,* vol. 229, pp. 1-17. https://doi.org/ 10.1016/j.enconman.2020.113744

[18] Alsadi S., Nassar Y., Ali K., (2016) General polynomial for optimizing the tilt angle of flat solar energy harvesters based on ASHRAE clear sky model in mid and high latitudes. Energy and Power;6(2):29-38. https://article.sapub.org/10.5923.j.ep.20160602.01.html

[19] Duffie, J. A., and Beckman, W. A., Solar Engineering of Thermal Processes, 4th ed., Wiley, New York. 2013.